New parametrization for unified dark matter and dark energy

Zahra Davari,[1,*] Mohammad Malekjani,[1,†] and Michal Artymowski[2,3,‡]

[1]*Department of Physics, Bu-Ali Sina University, Hamedan 65178, 016016, Iran*
[2]*Institute of Theoretical Physics, Faculty of Physics, University of Warsaw,
ul. Pasteura 5, 02-093 Warsaw, Poland*
[3]*Institute of Physics, Jagiellonian University, Łojasiewicza 11, 30-348 Kraków, Poland*

In this paper, we investigate a new phenomenological parametrization for unified dark matter and dark energy based on the polynomial expansion of the barotropic equation of state parameter *w*. Our parametrization provides a well-behaving evolution of *w* for both small and big redshifts as well as in the far future. The dark fluid described by our parametrization behaves for big redshifts like dark matter (DM). Therefore, one can parametrize dark energy and dark matter using a single dark fluid, like in the case of the Chaplygin gas. Within this parametrization, we consider two models: one with a dark energy (DE) barotropic parameter fixed to be −1 and the second one, where *w* ≠ −1 is chosen to match the best fit to the data. We study the main cosmological properties of these models at the expansion and perturbation levels. Based on the Markov chain Monte Carlo method with the currently available cosmic observational data sets, we constrain these models to determine the cosmological parameters at the level of the background and clustering of matter. We consider the interaction between dark matter and dark energy which directly affects the evolution of matter and its clustering. Our model appears to be perfectly consistent with the ΛCDM model, while providing unification of DE and DM.

I. INTRODUCTION

Various evidences from independent cosmic observations such as measurements of the rotation curves of spiral galaxies [1,2], dynamics of galaxy clusters [3], and cosmic structure formation [4] show that there is roughly 6 times more cold dark matter (CDM) than can be afforded by the baryonic matter in the cosmic matter budget making up of order ∼30% of critical density [5]. In addition to this clustering dark component, the astronomical observations including, e.g., supernovae type Ia (SNIa) [6–8], cosmic microwave background (CMB) fluctuations [5,9–11], large-scale structure (LSS) by the Sloan Digital Sky Survey (SDSS) [12], baryonic acoustic oscillation (BAO) [13–17], and galaxy clustering provide evidences for the existence of the so-called dark energy (DE)—an exotic fluid with sufficiently negative pressure, which causes the late-time accelerated expansion of the Universe.

Despite a lot of studies on dark matter (DM) and DE, their physical properties, origin, and nature are yet unknown. In literature, many candidates have been suggested for dark matter such as axions [18], the lightest supersymmetric particle (LSP) like neutralinos [19], and the KaluzaKlein particles [20] that are weakly interacting

massive particles (WIMPs) [21,22]. Also for DE, the most natural candidate is a cosmological constant with a constant equation of state (EoS) $w_\Lambda = -1$, but there is a discrepancy of some 120 orders of magnitude between its theoretical and observed values known as the fine-tuning problem [23–26]. For this reason, other candidates such as quintessence and k-essence models with a time varying EoS parameter have been suggested. Quintessence models involve canonical kinetic terms of the self-interacting scalar field [27], and k-essence models contain exotic scalar fields with noncanonical (nonlinear) kinetic terms which typically lead to a negative pressure. Generally speaking, it has been proposed that we cannot entirely understand the nature of DE before the establishment of a complete theory of quantum gravity [28]. One can ask if it is possible to obtain a simple model, in which a single dark fluid (DF) behaves as both dark matter and dark energy [29]. This attractive dark fluid with a barotropic equation of state (EoS) *w* (which is the ratio of pressure to energy density) can unify DM and DE and explain both the accelerated and decelerated expansions at late and early times, respectively. In other words, the barotropic EoS parameter of DF acts like a DM EoS parameter ($w_m \sim 0$) at high redshifts and behaves like a DE EoS parameter ($w_{de} < -1/3$) at low redshifts. This dual role of DF is the most interesting and surprising property in these scenarios. For this fluid, the coincidence problem of Λ*CDM* (i.e., why we live in a particular era during which

_____

*z.davaridolatabadi@sci.basu.ac.ir
†malekjani@basu.ac.ir
‡michal.artymowski@uj.edu.pl

both dark components are of the same order of magnitude at the present, whereas they were so different in most of the past evolution of the Universe) is resolved [30]. One particular case of DF which unifies DM and DE is the so-called generalized Chaplygin gas (gCg), introduced by Kamenshchik [31] and then developed in [32].

On the other hand, one possible way to study the EoS parameter of DE models is via parametrizations. In literature, we can find different EoS parametrizations for DE in which the EoS parameter of DE is defined as a function of cosmic redshift [$w(z)$]. The simplest and earliest EoS parametrizations are introduced based on the Taylor expansion of the EoS parameter of DE, w_{de}, with respect to redshift z as: $w_{de}(z) = w_0 + w_1 z$ [33,34] and with respect to $(1 - a)$ as: $w_{de}(z) = w_0 + w_1 \frac{z}{1+z}$, where $a = 1 + z$ is a scale factor of the FRW metric. The second parametrization is a well-known Chevallier-Polarski-Linder (CPL) parametrization proposed by [35,36]. In addition, some purely phenomenological parametrizations have been introduced in recent years. For instance, $w_{de}(z) = w_0 + w_1 z/(1 + z)^\gamma$, where γ fixes to 2 [37]. Moreover, the power law $w_{de}(a) = w_0 + w_1 (1 - a^\alpha)/\alpha$ and logarithmic $w_{de}(a) = w_0 + w_1 \ln a$ parametrizations have been suggested [38,39]. Another phenomenological parametrization is the Wetterich parametrization $w_{de}(z) = w_0/[1 + b \ln (1 + z)]^\alpha$, where α is fixed to 1 or 2 [40]. The important note is that although the CPL formula is a well-behaved parametrization at early ($a \ll 1$) and present ($a \sim 1$) epochs, it diverges when the scale factor goes to infinity at the far future. All of the above parametrizations are introduced to describe the evolution of the EoS parameter of DE. Based on our knowledge, there is still no specific parametrization to describe the barotropic EoS parameter of DF that consists of DM and DE. In this work, we introduce a new parametrization for the barotropic EoS parameter of DF (hereafter, *DF parametrization*). Using this parametrization (see Sec. II for a complete description), the barotropic EoS parameter of DF can tend to $w = 0$ at the early matter dominated Universe and $w < -1/3$ at the late time accelerated Universe. This paper is organized as follows. In Sec. II, we introduced the DF parametrization and study the evolution of its EoS parameter. In Sec. III, the cosmological background evolution based on the DF parametrization is investigated. We study the redshift evolution of the main cosmological quantities using DF parametrization. Using the latest cosmological data in a background level including data from joint light-curve analysis (JLA) supernovae, CMB, BAO, big bang nucleosynthesis (BBN), and Hubble expansion rate, in the context of a Markov chain Monte Carlo (MCMC) algorithm, we perform a joint likelihood statistical analysis in order to constrain the free parameters of DF parametrization. In Sec. IV, we investigate the growth of matter perturbations using DF parametrization and then perform a likelihood analysis using the growth rate of perturbations to place a constraint on the parameters of the model in the perturbation level and obtain their best fit values. Finally, we summarize our results in Sec. V.

II. DF PARAMETRIZATION

First, let us consider a simple parametrization for the barotropic EoS parameter of DF as

$$w(a) = w_0 + \sum_{n=1}^{N} w_n (1 - a)^n, \tag{1}$$

where a is scale factor normalized to 1 at present time, w_n are constant coefficients, and w_0 is a present-day barotropic parameter. The issue is that this parametrization leads to divergences of $w(a)$ in the far future, i.e., in the $a \to \infty$ limit. In principle, this is not an issue that would experimentally exclude the model. Quite obviously, one can only measure past values of w, so its future behavior cannot be a subject of experimental verification. Nevertheless, a parametrization with a nonstable w could be considered as decoupled from the predictions of most of the theoretical models of DE. Starting from DE models motivated by the field theory, like quintessence, to $f(R)$ and scalar-tensor theories, one usually obtains a rather constant value of the EoS parameter in the far future. Thus, a part of our motivation is to include in our analysis a connection between a phenomenological parametrization and more fundamental theories of DE. In order to solve the problem of an unstable w, one can secure the existence of finite and slowly evolving $w(a)$ for an arbitrary big, but finite value of a by assuming that $w(a)$ has a stationary point at some $a = a_s$. The maximal order of a stationary point in the case of Eq. (1) is equal to $N - 1$, which leads to $N - 1$ constraints on $w(a)$, namely,

$$\frac{dw}{da} = \frac{d^2 w}{da^2} = \ldots = \frac{d^{N-1} w}{da^{N-1}} = 0. \tag{2}$$

We have obtained $N - 1$ independent equations that constrain $N + 2$ parameters (including $N + 1$ different w_n and a_s), which gives three independent parameters of such a model. Note that this number is N independent. From Eqs. (1) and (2), one can find

$$a_s = \left(N \frac{w_N}{w_1} \right)^{\frac{-1}{N-1}}, \quad w_n = (-1)^{n+1} \frac{(N-1)!}{n!(N-n)!} \left(N \frac{w_N}{w_1} \right)^{\frac{n-1}{N-1}}. \tag{3}$$

For an arbitrary w_N, the barotropic EoS parameter $w(a)$ does not necessarily converge in the $N \to \infty$ limit. Note however that for

$$w_N = \sigma (w_1/N)^N, \tag{4}$$

where σ is any positive constant, one can obtain a $N \to \infty$ limit of the theory, which gives

$$w_N \to 0, \quad a_s \propto \frac{N}{w_1} \to \infty, \quad w(a) = w_0 + 1 - e^{-w_1(a-1)}. \quad (5)$$

This leaves us with two parameters of the theory. With a growing N, one obtains a bigger a_s, which secures a lack of divergence of $w(a)$ for bigger values of a. The $N \to \infty$ limit guarantees a lack of divergences for all a. It is easy to show that any barotropic EoS parameter $w(a)$ of the form

$$w(a) = w_0 + f(1 - e^{-w_1(a-1)}), \quad (6)$$

where $f(a)$ is continuous, differentiable, and well-defined function for all a, satisfies conditions (2) in the $N \to \infty$ limit. We have normalized the scale factor to be equal to 1 today, and we have assumed $f(a = 1) = 0$ in order to obtain w_0 as a present value of a barotropic parameter of DF. Such a theory may have an arbitrary number of free parameters within the $f(x)$ function. Again, let us emphasize that the infinite order stationary point in $a \to \infty$ secures a finite value of $w(a)$ for all values of the scale factor. Therefore, one avoids divergences of $w(a)$, which are otherwise present for this type of parametrization. Based on Eq. (6), let us assume one of the simplest forms of $f(a)$, namely,

$$w(a) = w_0 + \alpha(1 - e^{-w_1(a-1)}), \quad (7)$$

where α is a constant. According to Eq. (7), one can obtain the following three limits for the evolution of the barotropic parameter $w(a)$:

$$w(a) = \begin{cases} w_0 + \alpha(1 - e^{w_1}) & a \to 0 \\ w_0 & a \to 1 \\ w_0 + \alpha & a \to \infty \end{cases},$$

where $a \to 0$ ($a \to \infty$) represents the far past (future) of the Universe. Note that both $a \to 0$ and $a \to \infty$ limits lead to constant and finite values of $w(a)$, which are significantly different from each other. This leads to the rapid transition period between the phases of quasiconstant values of w, which has been investigated in the context of different parametrizations of inflation and DE in [41–45]. In principle, we want to obtain a smooth transition between some initial, almost constant value of the barotropic parameter denoted as $w_{\rm in}$ and a final one, which is $w_0 + \alpha$. In order to obtain such an evolution of w, let us note that for

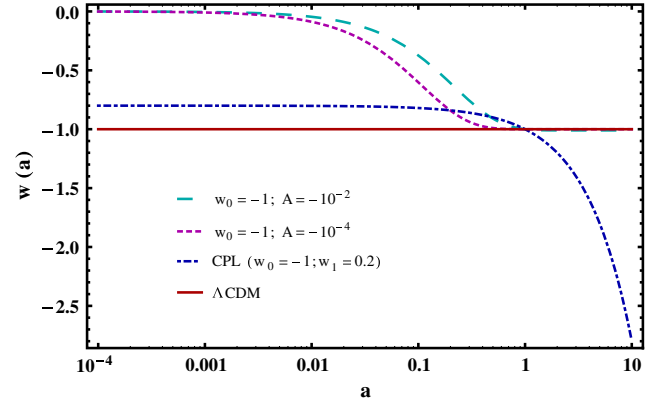$$w_1 = \log\left(\frac{w_0 + \alpha - w_{\rm in}}{\alpha}\right), \quad (8)$$

FIG. 1. The evolution of the EoS parameter of a unified DF and CPL parametrization as a function of scale factor a. The EoS parameter of CPL parametrization goes to infinity at the far future while the EoS parameter of unified DF coincides the ΛCDM one at today and future times.

one finds $w \to w_{\rm in}$ for $a \to 0$. In such a case from Eqs. (7) and (8), one finds the following form of the barotropic parameter:

$$w = w_0 + \left(1 - \left(\frac{w_0 + \alpha - w_{\rm in}}{\alpha}\right)^{1-a}\right). \quad (9)$$

In this paper, we investigate the case of $w_{\rm in} = 0$. Nevertheless, one could use this parametrization to describe the transition between a massless scalar field and DE (for $w_{\rm in} = 1$) [43] or between a radiationike evolution of a fluid and DE ($w_{\rm in} = 1/3$) [46]. Note that one needs $\alpha < 0$ in order to obtain those limits.

Based on Eq. (9), in Fig. 1, we show the evolution of the EoS parameter of DF $w(a)$ as a function of scale factor for $w_0 = -1$ and two different values of the free parameter α. Note that for our parametrization of $w(a)$, one can always find a, for which w vanishes, meaning that the barotropic parameter of the DF behaves as pressureless DM. On the other hand, at present and future times, $w(a)$ tends to -1, which means that DF acts like a cosmological constant. For comparison, we also show the EoS parameter of CPL parametrization and the constant EoS parameter of the ΛCDM model. We see that the CPL parametrization diverges when the scale factor goes to infinity at the far future.

III. DF PARAMETRIZATION AGAINST GEOMETRICAL OBSERVATIONS

In this section, we obtain the basic equations governing the evolution of background cosmology within DF parametrizations. Then using the observational data in the background level, we perform the statistical MCMC analysis to put constraints on the cosmological parameters in the context of DF parametrization. Finally, we show the

evolution of main cosmological quantities describing the evolution of background cosmology in DF parametrization.

A. Basic equations

In this section, we use Eq. (9) with $w_i = 0$ as a parametrization describing the barotropic EoS parameter of DF (denoted in here as DF parametrization) to study the evolution of Hubble flow in the spatially flat Friedman-Robertson-Walker (FRW) universe. We assume that the Universe is filled with baryonic matter, radiation, and unified DF. Then, the first Friedmann equation takes the following form:

$$H^2 = \frac{1}{3m_p^2}(\rho_b + \rho_r + \rho_{df}),\tag{10}$$

where $m_p^2 = \frac{1}{8\pi G}$ is the reduced Planck mass and ρ_b, ρ_r, and ρ_{df} are the energy densities of baryons, radiation, and DF, respectively. In the absence of interactions among the above fluids, the evolution of the energy density as a function of the cosmic scale factor $a(t)$ is characterized by the continuity equation as follows:

$$\frac{d\rho_i}{da} + \frac{3}{a}(1 + w_i(a))\rho_i = 0,\tag{11}$$

where $\rho_i(a)$ is the energy density of radiation ($w_i = 1/3$), baryonic matter ($w_i = 0$), and DF is given via Eq. (9), respectively. It is easy to derive the evolution of the energy density of baryons and radiation as $\rho_b = \rho_{b0}a^{-3}$ and $\rho_r = \rho_{r0}a^{-4}$, respectively. Also inserting Eq. (9) into Eq. (11), we can obtain the evolution of ρ_{df} as

$$\rho_{df}(a) = \rho_{df0}e^{-3\int_1^a \frac{1+w(x)}{x}dx}.\tag{12}$$

Using the definition of the dimensionless energy density parameter $\Omega_i = \frac{\rho_i}{\rho_{cr}}$, where $\rho_{cr} = 3m_p^2 H^2$ is the critical energy density, the dimensionless Hubble parameter, $E = \frac{H}{H_0}$ takes the following form:

$$E = \sqrt{\Omega_{b0}a^{-3} + \Omega_{r0}a^{-4} + \Omega_{df0}e^{-3\int_1^a \frac{1+w(x)}{x}dx}}.\tag{13}$$

Applying the Friedman equation, which takes the form of $\sum \Omega_i = 1$, we can write $\Omega_{df0} = 1 - \Omega_{b0} - \Omega_{r0}$, where $\Omega_{r0} = 2.469 \times 10^{-5}h^{-2}(1.6903)$ is the energy density of radiation (photons + relativistic neutrinos) and $h = H_0/100$ [47]. Notice that in the case of our model, DF is considered as the unification of DM and DE and therefore, the DM energy density is not explicitly included in the Hubble flow. In order to obtain the evolution of DM and DE separately, one needs to decompose the energy density of DF as

$$\rho_{df} = \rho_{dm} + \rho_{de}.\tag{14}$$

According to the energy-momentum conservation equation, one obtains the continuity equation for DF as

$$\dot{\rho}_{df} + 3H(1 + w)\rho_{df} = 0.\tag{15}$$

Then, the continuity equations for DM and DE are, respectively, given by

$$\dot{\rho}_{dm} + 3H\rho_{dm} = Q,\tag{16}$$

$$\dot{\rho}_{de} + 3H(1 + w_{de})\rho_{de} = -Q,\tag{17}$$

where Q is the interaction parameter between DM and DE ([48–50]). Note, that unified models of DM and DE have a certain issue related to the behavior of the speed of sound, namely, they may lead to the production of unphysical oscillations [51]. The unified models behave like DM at early times, and therefore their sound speed is vanishing. As one approaches the present time, the unified models behave like DE with a negative pressure resulting in a large sound speed, which produces oscillations or blowup in the power spectrum [51]. In unified models, this is an unavoidable feature unless we identify the DM and DE components of one fluid. In our case, it is natural to assume that DM and DE are interacting as they are both considered as a single fluid. Because of the interaction, one obtains a dissipation of energy between DM and DE, which can be estimated phenomenologically as [52,53]

$$Q = 3aH(\xi_1 \rho_{dm} + \xi_2 \rho_{de}),\tag{18}$$

where ξ_1 and ξ_2 are the coupling coefficients, and they can be determined by observations. The energy flow from DE to DM is defined by $Q > 0$, and oppositely $Q < 0$ shows the energy flow from DM to DE.

Using Eq. (14) and the barotropic equation for DF $P_{df} = w(a)\rho_{df}$, assuming $P_{df} = P_{de}$ (since $P_{dm} = 0$), we can obtain $\rho_{dm} = (\frac{w_{de}(a)-w(a)}{w_{de}(a)})\rho_{df}$ and $\rho_{de} = \frac{w(a)}{w_{de}(a)}\rho_{df}$. Hence, the dimensionless energy densities of DM and DE can be obtained as: $\Omega_{dm} = \frac{w_{de}(a)-w(a)}{w_{de}(a)}\Omega_{df}$ and $\Omega_{de} = \frac{w(a)}{w_{de}(a)}\Omega_{df}$. The energy density of DM and DE can be obtained as follows:

$$\Omega_{dm} = \frac{\Omega_{df0}(w_{de} - w(a))e^{-3\int_1^a \frac{1+w(x)}{x}dx}}{w_{de}E^2(a)},\tag{19}$$

$$\Omega_{de} = \frac{\Omega_{df0}w(a)e^{-3\int_1^a \frac{1+w(x)}{x}dx}}{w_{de}E^2(a)}.\tag{20}$$

In the rest of paper, we consider two different cases for DE. First, we assume DE as a cosmological constant with

TABLE I. Best fit values of cosmological parameters obtained in MCMC analysis using the geometrical data in the background level.

Parameter	Case 1	Case 2	ΛCDM
Ω_{b0}	$0.050^{+0.0008+0.002}_{-0.0008-0.002}$	$0.051^{+0.0008+0.002}_{-0.001-0.002}$	$0.049^{+0.0008+0.002}_{-0.0008-0.002}$
H_0	$68.9^{+0.64+1.3}_{-0.64-1.2}$	$68.36^{+0.65+1.3}_{-0.65-1.3}$	$69.2^{+0.69+1.4}_{-0.69-1.3}$
w_0	$-0.73^{+0.008+0.02}_{-0.008-0.02}$	$-0.69^{+0.02+0.04}_{-0.02-0.05}$	$\cdots$
α	-51.3^{+13+22}_{-11-25}	$-39.1^{+8.0+9.5}_{-8.4-11}$	0
w_{de}	-1	$-0.95^{+0.02+0.05}_{-0.03-0.05}$	-1
Ω_{dm0}	0.257	0.263	$0.246^{+0.008+0.02}_{-0.008-0.02}$
Ω_{de0}	0.693	0.686	0.705

$w_{de} = -1$ (case 1). Second, we consider DE as a quintessence model with a constant w_{de} that differs from -1 (case 2) in order to provide the best fit to the data (see Table I for details). Let us note that both cases are considered within the parametrization of the DF presented in the Eq. (9).

B. Geometrical observations and cosmological constraints

Now using the background expansion data including those of a JLA supernovae binned sample [54,55], BAO [17,56–58], Planck data for the position of CMB acoustic peak [59], BBN [60], Hubble data [17,58,61,62], we implement a statistical MCMC analysis for the two classes of DF parametrization described in Sec. III A. For more details regarding the MCMC method used in this work, we refer the reader to [63] [see also [47,64–67]]. In this section, we have used the following sets of data: 31 distinct points for JLA binned sample data, 37 points for Hubble data [see Table 3 of [68]]. The BAO data include six distinct measurements of the baryon acoustic scale [see Table 1 of [63]]. We use the Plank data for the position of CMB acoustic peak in [59]. The big bang nucleosynthesis (BBN) provides the data point which constrains $\Omega_b^{(0)}$ [60]. The total likelihood function is the product of the individual likelihoods for each experiment as

$$\mathcal{L}_{tot}(\mathbf{p}) = \mathcal{L}_{sn} \times \mathcal{L}_{bao} \times \mathcal{L}_{cmb} \times \mathcal{L}_{h} \times \mathcal{L}_{bbn}, \quad (21)$$

so the total chi-square (χ^2_{tot}) is given by the sum of the individual chi-squares,

$$\chi^2_{tot}(\mathbf{p}) = \chi^2_{sn} + \chi^2_{bao} + \chi^2_{cmb} + \chi^2_{h} + \chi^2_{bbn}, \quad (22)$$

where the statistical vector p contains free parameters of the cosmological model. This vector for ΛCDM cosmology contains $\{\Omega_{b0}, \Omega_{dm0}, H_0\}$. For DF parametrization (case 1), the vector p contains $\{\Omega_{b0}, H_0, w_0, \alpha\}$, and for DF parametrization (case 2), the vector p includes $\{\Omega_{b0}, H_0, w_0, \alpha,$

$w_{de}\}$. Notice that in the case 2, we have one more free parameter (w_{de}) than case 1, since in the case 2, we consider DE as a quintessence with an unknown EoS parameter w_{de}, while in case 1, DE is considered as a cosmological constant Λ with a constant EoS $w_{\Lambda} = -1$. In this analysis, we fix the energy density of radiation (photons + relativistic neutrinos) as $\Omega_{r0} = 2.469 \times 10^{-5}h^{-2}(1.6903)$, where $h = H_0/100$ [47].

In the chi-square analysis, it is clear to conclude that a model with a lower value of χ^2_{min} is better fitted to observational data compared to other models. However, this result is valid if the number of free parameters of models are equal. In other words, this analysis is no longer valid for comparing different models with a different number of free parameters. Hence, we use other statistical tests, the so-called Akaike information criteria (AIC) and Bayesian information criterion (BIC) to compare DF parametrizations with observations. Notice that in ΛCDM cosmology, we have three free parameters; in the case of DF parametrization (case 1), there are four free parameters, and in case (2), we have five free parameters. The AIC [69,70] and BIC [71] estimators are defined as

$$AIC = -2\ln \mathcal{L}_{max} + 2k + \frac{2k(k+1)}{N-k-1}, \quad (23)$$

$$BIC = -2\ln \mathcal{L}_{max} + k\ln N, \quad (24)$$

where $\mathcal{L}_{max}$ is the highest likelihood function (proportional to a minimum of χ^2), N is the number of observational data, and k is the number of free parameters. One can ignore the last term in the rhs of Eq. (23) when the number of observational data N is much more than the number of free parameters k. Among all models, the one that minimizes the AIC is considered to be the best one. If the difference between the AIC of a given model and the best model is smaller than 4 ($\Delta = AIC_{model} - AIC_{min} < 4$), one concludes that the best fitted model and a given model are equally supported by the data. In the case of $4 < \Delta < 10$, observations still support the given model but less than the best one. Finally, for $\Delta > 10$, observations basically do not support the given model comparing to the best model. The results of our analysis are presented as follows:

  (i) DF parametrization (case 1): $\chi^2_{min} = 65.8$, $k = 4$, $AIC = 74.35$.
  (ii) DF parametrization (case 2): $\chi^2_{min} = 62.21$, $k = 5$, $AIC = 73.04$.
  (iii) ΛCDM model: $\chi^2_{min} = 69.94$, $k = 3$, $AIC = 76.26$.

The above results show that the DF parametrization (case 2) has the lowest value of AIC. However, since the difference between the two cases of DF parametrization is about 1.3, we conclude both DF parametrizations are equally fitted to the observational data in the background level. Furthermore, we see that the difference between the AIC value of
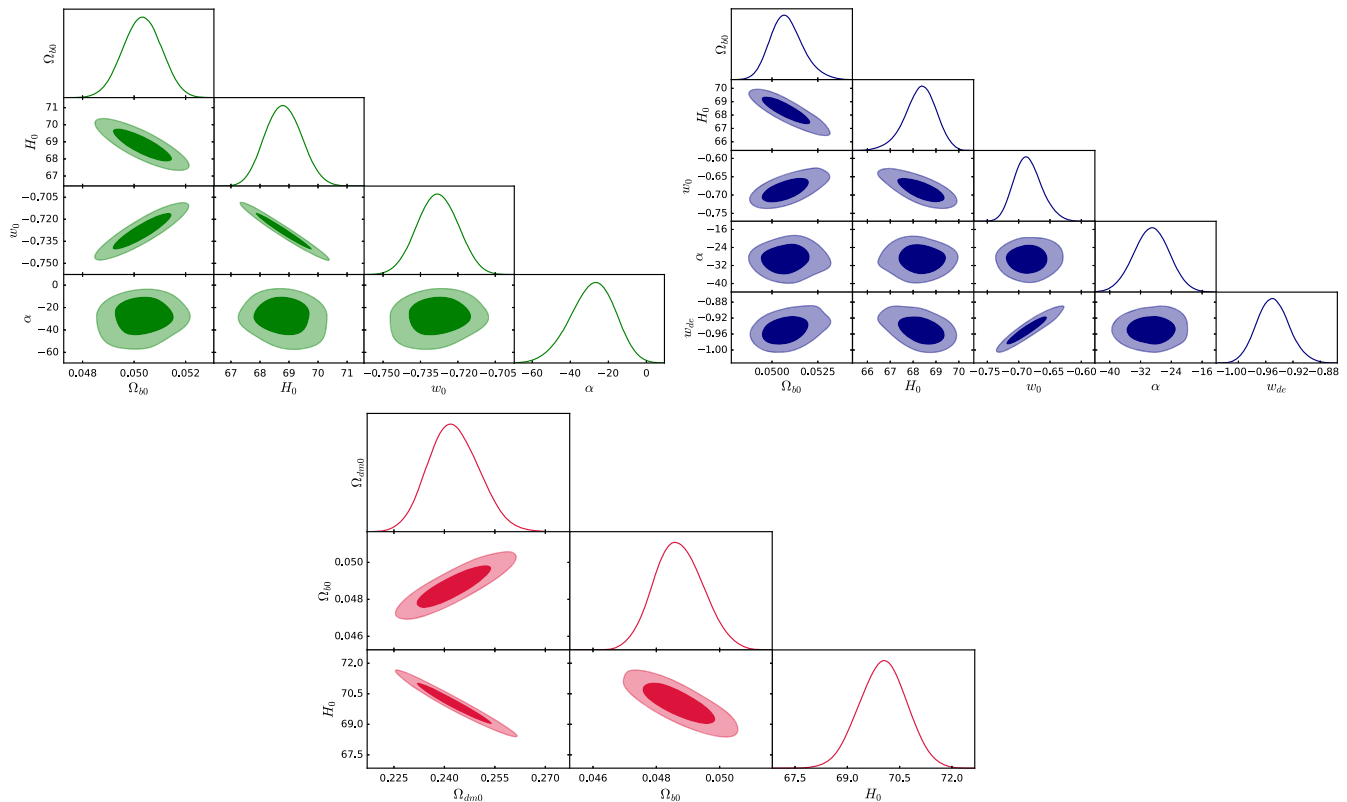
FIG. 2.   The 1σ and 2σ confidence levels and maximum likelihood function for various cosmological parameters planes. Upper left (upper right) panel stands for case 1 (case 2) and bottom panel stands for ΛCDM cosmology.

ΛCDM cosmology and DF parametrization (case 2) is less than 4. Hence, all models studied in this work are well fitted to the observational data in the background level. The best fit values of cosmological parameters are presented in Table I. Also, 1σ and 2σ confidence levels of cosmological parameters are shown in Fig. 2.

C. Cosmological evolution

In this section, based on the best fit values of cosmological parameters presented in Table I, we depict the evolution of the main cosmological quantities in the framework of DF parametrization. In Fig. 3, we present the evolution of the fractional energy densities for radiation, DM, and DE. For all models, the Universe evolves from a radiation dominated phase to a matter dominated epoch and finally, enters the late time DE dominated phase. The radiation-matter equality epoch for ΛCDM model occurs at $a_{\rm eq} \approx 2.9 \times 10^{-4}$. For DF parametrization case 1 (case 2), it happens later at $a_{\rm eq} \approx 5.5 \times 10^{-4} (a_{\rm eq} \approx 5.1 \times 10^{-4})$. In all models, we see that DE starts to dominate the energy budget of the Universe at $a \sim 0.75$. Notice that in the case of DF parametrization, due to the interaction between DM and DE, the evolution of energy density of both DM and DE is different from the one in the ΛCDM scenario.

In Fig. 4, we show the evolution of the EoS parameter of DF w, the Hubble parameter E, and deceleration parameter q as a function of redshift z. Notice that in case 2, we use the best fit values for cosmological parameters based on
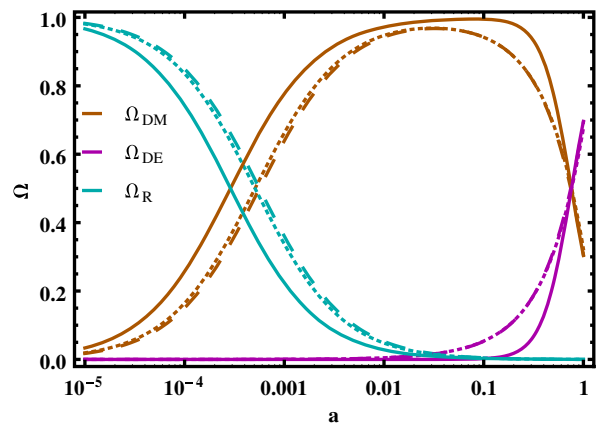

FIG. 3.   Evolution of the fractional energy density of radiation (green curves), nonrelativistic matter (brown curves), and DE component (pink curves) in terms of a cosmic scale factor for different DF parametrizations and standard ΛCDM cosmology. Dashed and dotted curves stand for case 1 and case 2 of DF parametrization, respectively. The solid curves represent the concordance ΛCDM model. In all models, we use the best fit values from Table I.
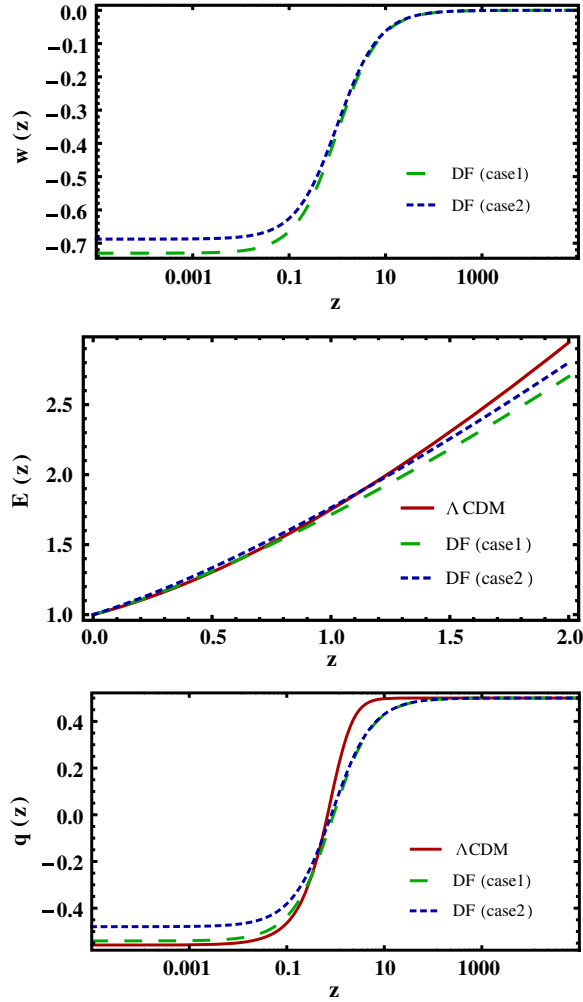
FIG. 4. Top panel: Redshift evolution of EoS parameter, w, of DF parametrizations. Middle panel: redshift evolution of Hubble parameter E. Bottom panel: redshift evolution of deceleration parameter q. In all panels, case 1 and case 2 are shown with dashed and dotted curves, respectively. The concordance ΛCDM cosmology is shown by red solid curve.

Table I. In the top panel, for both cases, we observe that the EoS parameter of DF tends to zero at high redshifts representing the pressureless matter fluid $w_m = 0$ at a high redshift Universe. While the redshift decreases, the EoS parameter decreases and reaches negative values smaller than $-1/3$, which is a necessary condition for DF to behave as DE at late times. In the middle panel, the redshift evolution of the Hubble parameter E has been shown for both cases of DF parametrization. The ΛCDM case is shown for comparison. We see that at high redshifts, the Hubble parameter for DF parametrizations is smaller than the ΛCDM case. However at low redshifts, the Hubble parameter in DF parametrization (case 1) coincides with the ΛCDM model. This result is expected since we assume the DE component of DF is a cosmological constant Λ with $w_{de} = -1$. At low redshifts, when the DE component of the DF dominates its evolution, we expect that the Hubble

parameter in DF (case 1) fits to the one from the ΛCDM cosmology. On the other hand, we observe that at low redshifts, the Hubble parameter in case 2 is a little larger than the ΛCDM cosmology. This is due to fact that we consider the DE part of DF as a quintessence DE with $w_{de} > -1$. Finally in the bottom panel, we present the evolution of a deceleration parameter $q(z) = -1 - \frac{\dot{H}}{H^2}$ for ΛCDM and DF parametrizations. The connection between $q(z)$ and w_{de} is rather straightforward. From the Friedmann equations, one finds

$$\frac{\dot{H}}{H^2} = -\frac{3}{2}(1 + w_{de}(z)\Omega_{de}(z)), \tag{25}$$

which implies that

$$q(z) = \frac{1}{2} + \frac{3}{2}w_{de}(z)\Omega_{de}(z). \tag{26}$$

In both ΛCDM model and DF parametrizations, q tends to $\frac{1}{2}$ at early times as expected. By solving the $q(z_{tr}) = 0$, we can obtain the transition redshift, namely the epoch at which the expansion of the Universe starts to accelerate. In particular, we find $z_{tr} = 0.9$ for DF parametrization (case 1), $z_{tr} = 0.87$ for DF parametrization (case 2), and $z_{tr} = 0.66$ for ΛCDM. Hence, the ΛCDM model is entering the accelerating phase later than DF parametrizations. These results are in good agreement with the measured z_{tr} based on the cosmic $H(z)$ data [72] [see also [73,74]].

IV. GROWTH OF PERTURBATIONS

Besides the observational data in the background level, it is important to study the features of different DE models using the observations in cluster scales. In fact, most of the dynamical DE models introduced as parallel candidates of Λ have the same behaviors at background cosmology. However, they may have a different evolution in cluster scales where we study the growth history of perturbations. Therefore, the information from large scale structure formation is a powerful tool to examine different types of DE models. In this section, we start from presenting the basic equations for the growth of matter perturbations in DF scenarios followed by the examination of the DF parametrizations against the observational growth rate data in the perturbation level.

A. Basic equations

We consider the scalar perturbations, which are developed at low redshifts in the era of structure formation. The perturbed line element in the conformal Newtonian gauge as

$$ds^2 = a^2(\tau)[-(1 + 2\psi)d\tau^2 + (1 - 2\phi)\delta_{ij}dx^i dx^j], \tag{27}$$

where x is the spatial coordinates and ψ and ϕ are the linear gravitational potentials. In the limit of General Relativity

and in the absence of anisotropic stresses, one finds $\psi = \phi$. We use Latin letters $i, j, \ldots$ for the spatial indexes 1, 2, 3, and Greek letters $\mu, \nu, \ldots$ for indexes 0, 1, 2, and 3. In this formalism, metric is given by

$$g_{\mu\nu} = a^2 \begin{pmatrix} -(1 + 2\psi) & 0 \\ 0 & (1 - 2\phi)\delta_{ij} \end{pmatrix}. \quad (28)$$

We can rewrite the perturbed metric in Eq. (28) by separating $h_{\mu\nu}$ as $g_{\mu\nu} = \bar{g}_{\mu\nu} + h_{\mu\nu}$, where $\bar{g}_{00} = -a^2$, $\bar{g}_{ij} = a^2\delta_{ij}$ are the metric components describing the background and $h_{00} = -2a^2\phi$, $h_{ij} = -2a^2\phi\delta_{ij}$ are the perturbations of metric [52]. The energy-momentum tensor for a perfect fluid in an homogeneous and isotropic universe reads

$$\bar{T}_{\mu\nu} = \bar{P} \, \bar{g}_{\mu\nu}(\bar{\rho} + \bar{P})\bar{u}_\mu\bar{u}_\nu, \quad (29)$$

where, u_μ is the four velocity. Let us decompose the energy-momentum tensor into $T_{\mu\nu} = \bar{T}_{\mu\nu} + \delta T_{\mu\nu}$, where $\bar{T}_{\mu\nu}$ and $\delta T_{\mu\nu}$ are background and perturbations, respectively. The perturbed part of the energy momentum tensor is the following:

$$\delta T_{\mu\nu} = (\delta\rho + \delta p)\bar{u}_\mu\bar{u}_\nu + (\bar{\rho} + \bar{P})(\delta u_\mu\bar{u}_\nu + \bar{u}_\mu\delta u_\nu) - \delta p\delta_{\mu\nu}, \quad (30)$$

where different nonzero components of Eq. (30) are obtained as

$$\begin{aligned} \delta T^0_0 &= -\delta\rho, & \delta T^i_j &= \delta p\delta^j_i, & \delta T_{00} &= a^2(\delta\rho + 2\bar{\rho}\phi), \\ \delta T^i_0 &= -a^{-1}(\bar{\rho} + \bar{P})\delta u^i, & \delta T^0_i &= a^{-1}(\bar{\rho} + \bar{P})\delta u_i, \\ \delta T_{0i} &= \delta_{i0} = -a(\bar{\rho} + \bar{P})\delta_i, & \delta T_{ij} &= a^2(\delta p - 2\bar{p}\phi)\delta_{ij}, \end{aligned} \quad (31)$$

where the bars indicate that the quantities are unperturbed. Using the perturbed metric $g_{\mu\nu}$ and the perturbed conservation equations, we can obtain the following evolution equation for the evolution of the matter perturbations [52,75]:

$$-\dot{\delta} - \left[3\mathcal{H}(c_s^2 - w_{\mathrm{de}}) - \frac{\bar{Q}_0}{\rho}\right]\delta - (1 + w_{\mathrm{de}})(\theta - 3\dot{\phi}) = \frac{\delta Q_0}{\rho},$$

$$\dot{\theta} + \left[\mathcal{H}(1 - 3w_{\mathrm{de}}) - \frac{\bar{Q}_0}{\rho} + \frac{\dot{w}_{\mathrm{de}}}{1 + w_{\mathrm{de}}}\right]\theta - k^2\phi - \frac{c_s^2 k^2}{1 + w_{\mathrm{de}}}\delta$$

$$= \frac{ik^i\delta Q_i}{\bar{\rho}(1 + w_{\mathrm{de}})}, \quad (32)$$

where the overdot is a derivative with respect to conformal time, $\delta \equiv \delta\rho/\bar{\rho}$ is the density perturbation, $c_s^2 \equiv \delta_p/\delta\rho$ is the sound speed of the DE, k^i are the component of the wave vector in Fourier space, $\theta \equiv a^{-1}ik^j\delta u_j$ is the divergence of the velocity perturbation in Fourier space, δQ_i are

the perturbation of the exchange of energy momentum in the perturbed conservation equations, and $\mathcal{H}$ is the conformal Hubble parameter. Notice that $\bar{Q}_0$ in above equation is the exchange of energy between DM and DE at the background level, and due to the homogeneity and isotropy of the Universe at the background level, its spatial components are zero [see also Eq. (18)].

Using the perturbed Poisson equation in the Fourier space, one finds

$$\left(1 + \frac{3\mathcal{H}^2}{k^2}\right)k^2\phi = -3\mathcal{H}\dot{\phi} - 4\pi Ga^2(\rho_m\delta_m + \rho_{\mathrm{de}}\delta_{\mathrm{de}}), \quad (33)$$

where δ_m is the density perturbation of pressureless matter (baryons + dark matter) and δ_{de} is the DE density perturbation. We focus on the growth of perturbations with a wavelength much smaller than the horizon ($k \gg \mathcal{H}$). In this limit, we can use the pseudo-Newtonian cosmology and neglect the time variation of gravitational potential. Hence, we can ignore the second term of the left-hand side of Eq. (33) and the term proportional to $\dot{\phi}$ at the right-hand side. Also due to the large sound horizon of DE, the DE perturbations ($\delta_{\mathrm{de}} = 0$) are expected to be negligible on subhorizon scales [76]. Therefore, the Poisson equation reduces to

$$k^2\phi = -4\pi Ga^2\rho_M\delta_m = -\frac{3}{2}\mathcal{H}^2\Omega_m\delta_m, \quad (34)$$

where $\Omega_m = \Omega_{\mathrm{dm}} + \Omega_b$ is the sum of fractional density parameter of dark matter and baryons. Combining Eq. (32) with the Poisson equation (34), we get

$$\dot{\delta}_m + 3\mathcal{H}\xi\frac{\Omega_{\mathrm{de}}}{\Omega_m}\delta_m + \theta_m = 0$$

$$\dot{\theta}_m + \mathcal{H}\left(1 + 3\xi\frac{\Omega_{\mathrm{de}}}{\Omega_m}\right)\theta_m + \frac{3}{2}\mathcal{H}^2\Omega_m\delta_m = 0. \quad (35)$$

Notice that here we use the reduced form of the phenomenological equation (18) as $Q = \bar{Q}_0 = -3\xi\mathcal{H}\rho_{\mathrm{de}} = -3\xi\mathcal{H}\frac{\Omega_{\mathrm{de}}}{\Omega_m}\rho_m$, by setting $\xi_1 = 0$. Since we are neglecting DE clustering, we also ignore perturbations of Q to derive Eqs. (35) [see also [52]]. By eliminating θ_m from the system of Eq. (35) and changing the variables from conformal time to physical time according to $\mathcal{H} = aH$, $\frac{d}{d\tau} = a\frac{d}{dt}$ and $\frac{d^2}{d\tau^2} = a^2(\frac{d^2}{dt^2} + H\frac{d}{dt})$, we obtain the following equation:

$$\frac{d^2\delta_m}{dt^2} + 2\left(H + 3\xi\frac{\Omega_{\mathrm{de}}}{\Omega_m}\right)\dot{\delta}_m - \frac{3}{2}H^2\left[\Omega_m - 2\xi\frac{\Omega_{\mathrm{de}}}{\Omega_m}\right.$$

$$\left. \times \left(1 + \frac{\dot{H}}{aH^2} + 3\xi\frac{\Omega_{\mathrm{de}}}{\Omega_m} - \frac{\dot{\Omega}_{\mathrm{de}}}{H\Omega_m\Omega_{\mathrm{de}}}\right)\right]\delta_m = 0. \quad (36)$$

Changing the time derivative into a derivative with respect to the scale factor a ($\frac{d}{dt} = aH\frac{d}{da}$), we get

TABLE II.   Numerical results for different DF parametrizations and the ΛCDM model obtained from the statistical MCMC analysis using the cosmological growth rate data in cluster scales. The best fit values of cosmological parameters ξ and $\sigma_8(z=0)$ with their 1σ and 2σ confidence levels are shown in the two first rows. The minimum of least square function χ^2 and minimum of AIC value are shown in two last rows.

Parameter	Case 1	Case 2	ΛCDM
$\xi(10^{-4})$	$7.2^{+0.003+0.006}_{-0.003-0.006}$	$7.3^{+0.17+0.3}_{-0.17-0.3}$	0
σ_8	$0.802^{+0.016+0.02}_{-0.015-0.02}$	$0.81^{+0.02+0.03}_{-0.02-0.04}$	$0.74^{+0.02+0.03}_{-0.02-0.04}$
$\chi^2_{\min}$	7.87	7.68	8.11
$AIC_{\min}$	12.51	12.31	10.31

$$\delta''_m + A_m \delta'_m + B_m \delta_m = S_m, \qquad (37)$$

where coefficients A_m, B_m, and S_m are written as

$$A_m = \frac{3}{a} + \frac{H'}{H} + \frac{6\xi}{a}\frac{\Omega_{de}}{\Omega_m};$$

$$B_m = -\frac{3}{2a^2}\left[-2\xi\frac{\Omega_{de}}{\Omega_m}\left(1 + \frac{H'}{H} + 3\xi\frac{\Omega_{de}}{\Omega_m} - \frac{\Omega'_m}{\Omega_m\Omega_{de}}\right)\right]$$

$$S_m = -\frac{3}{2a^2}\Omega_m\delta_m. \qquad (38)$$

Notice that by putting $\xi = 0$, the standard equation for the evolution of matter perturbations can be recovered. Now we numerically solve Eq. (37) to obtain the evolution of the growth of matter perturbations in DF cosmology. Concerning the initial conditions, we set the initial scale factor $a_i = 0.0005$ ($z_i = 2000$), which means that we are deep enough in the early matter dominated era. We use $\delta_{mi} = 8 \times 10^{-5}$, which guarantees that the linear regime ($\delta_m < 1$) of perturbations at the present time. The background cosmological parameters have been used from the best fit values presented in Table I. In addition, we set the interaction parameter ξ to the constrained value $\xi = 7 \times 10^{-4}$ obtained in Table II. Once the matter perturbation $\delta_m(z)$ is obtained, we calculate the

evolution of the growth rate function $f = \frac{d\ln\delta_m}{d\ln a}$ and the mass variance of matter perturbations σ_8 within the sphere of $R_8 = 8h^{-1}Mpc$. The variance of perturbations within R_8 at redshift z reads $\sigma_8(z) = D(z)\sigma_8(z=0)$, where $D(z) = \delta_m(z)/\delta_m(z=0)$ is the linear growth factor of matter perturbations and $\sigma_8(z=0)$ is the present value of variances. For models discussed in this work, we fix $\sigma_8(z=0)$ from the constrained values in Table II.

In the left panel of Fig. 5, we show the evolution of the growth rate function f as a function of the cosmic redshift z. One can see that DE decreases the amplitude of matter perturbations at low redshift. We observe that in both cases of DF models and concordance ΛCDM cosmology, the growth rate of matter perturbations is suppressed due to the effect of a DE component at low redshifts. Notice that at high redshifts, the influence of DE on the growth of perturbations is negligible, and consequently, the growth function goes to unity, which corresponds to the matter dominated Universe. We conclude that the suppression of the amplitude of matter fluctuations in DF cosmologies starts sooner comparing to the standard ΛCDM model. This result can be extracted from Fig. 2 in which the fractional energy density of DE at higher redshifts calculated in ΛCDM model vanishes sooner than in the case of DF cosmology. Hence, the nonvanishing DE at higher redshifts suppresses the growth of matter fluctuations at earlier times.

In the right panel of Fig. 5, we show the evolution of $\sigma_8(z)$ as a function of redshift z computed for DF and ΛCDM models. Note, that the variance of perturbations in both DF cosmologies and the ΛCDM model grows with a scale factor. Moreover, opposite to the behavior of growth rate function, the variance of perturbations in DF models is larger than the one in the case of the ΛCDM universe.

B. Growth rate data

In this section, we calculate the theoretical value of $f(z)\sigma_8(z)$ in the context of DF cosmology. Using the
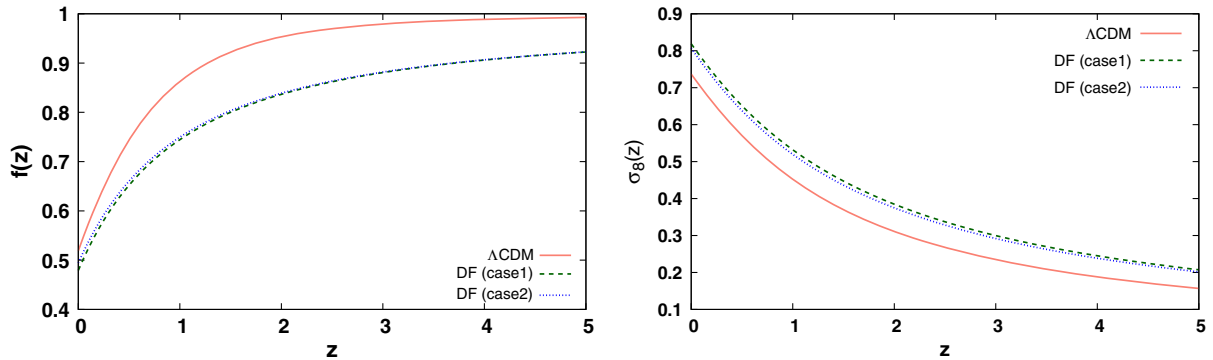

FIG. 5.   Redshift evolution of matter growth rate function $f(z)$ (left panel) and variance of perturbations σ_8 (right panel) in the context of DF cosmology. The background cosmological parameters are fixed using their values obtained in Table I. The interaction parameter ξ and $\sigma_8(z=0)$ are fixed using their constrained values in Table II. The concordance ΛCDM cosmology is shown by solid curve.
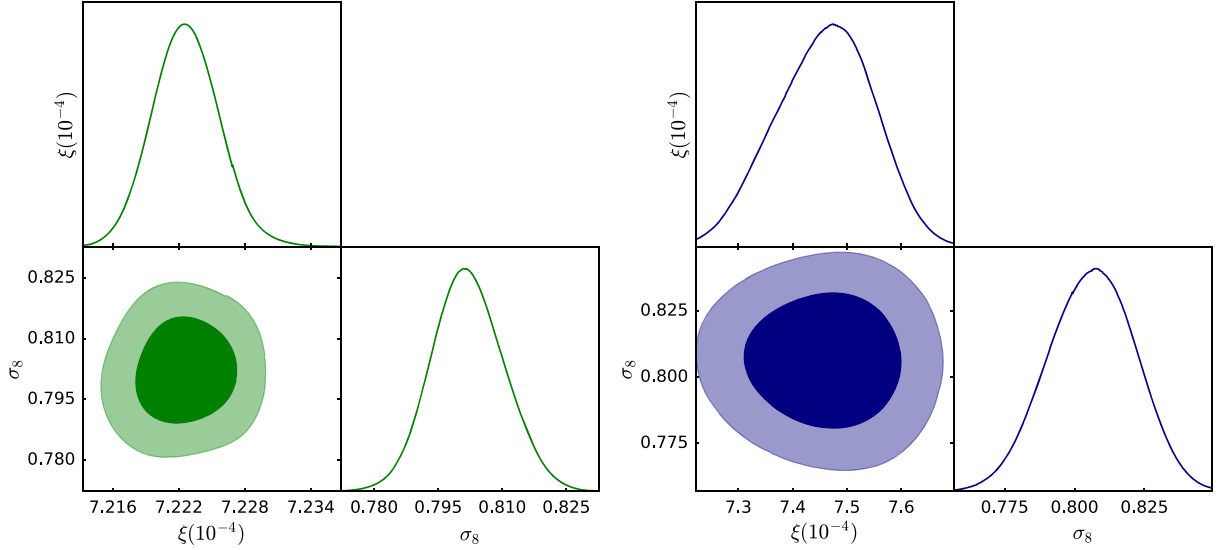
FIG. 6.   The 1σ and 2σ confidence contours and maximum likelihood functions in $\xi - \sigma_8(z=0)$ plane for case 1 (left panel) and case 2 (right panel) of DF parametrization.

observational growth rate data [77], we perform a statistical least square analysis to compute

$$\chi^2_{\text{gr}} = \Sigma^N_{i=1} \frac{[f\sigma_8^{(th)}(z_i) - f\sigma_8^{(obs)}(z_i)]}{\sigma_i^2}, \qquad (39)$$

where σ_i are corresponding uncertainties, "obs" stands for the observed data, and "th" denotes the theoretical prediction in DF cosmology. The growth rate data used in this analysis comes from 18 distinct data points for $f\sigma_8(z)$ [77]. Here, we consider the interaction parameter ξ and mass variance $\sigma_8(z=0)$ as free parameters, which can be constrained by growth rate data. We fix the other cosmological parameters using the best fit values presented in Table I. In MCMC analysis (performed using the growth
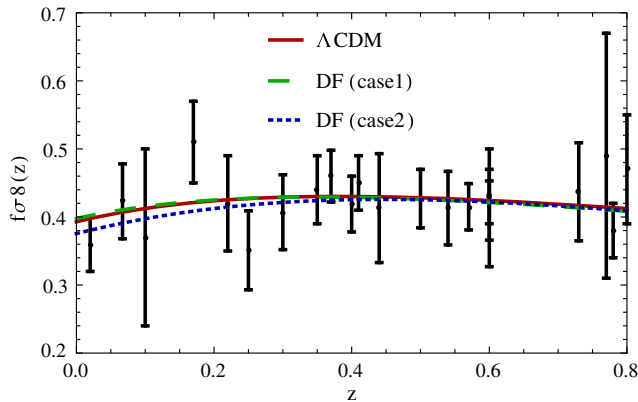

FIG. 7.   Theoretical predicted $f(z)\sigma_8(z)$ using the best fit values of cosmological parameters in Tables I and II compared to observational growth rate data points. DF parametrizations case 1 and case 2 are shown by dashed and dotted curves, respectively. The concordance ΛCDM cosmology is shown by red solid curve.

rate data), the statistical vector p contains two free parameters [ξ, $\sigma_8(z=0)$] for DF cosmology (both case 1 and 2) and $\sigma_8(z=0)$ for concordance ΛCDM cosmology. Our results in this analysis are presented in Table II. We show that the ΛCDM model, which appears to have the lowest AIC value, is the best model in cluster scales. However, since the difference between AIC of DF parametrizations (both case 1 and 2) and the ΛCDM model is lower than 3, we conclude that both cases of DF parametrizations are fitted to growth rate data as well as in the case of the ΛCDM cosmology. In Fig. 6, we visualize the 1σ and 2σ confidence levels in $\xi - \sigma_8$ plane for the DF parametrization case 1 (left panel) and for case 2 (right panel). In Fig. 7, we show the theoretically predicted $f(z)\sigma_8(z)$ for DF parametrizations using the best fit cosmological parameters presented in Tables I and II. We see that both DF parametrizations are well fitted with observational growth rate data and that the fit is as good as in the case of ΛCDM cosmology. This result is comparable with the implications of Fig. 5, in which the predicted growth rate function $f(z)$ in DF cosmologies is lower than that in the ΛCDM model (see left panel), while the quantity $\sigma_8(z)$ calculated in DF models is higher than the same quantity in the ΛCDM universe (right panel). Hence, one can conclude that the production of the growth rate function and variance of perturbation, i.e., $f(z)\sigma_8(z)$, of DF cosmology is compatible with that of the one in the ΛCDM model (see Fig. 7).

V. CONCLUSION

In this paper, we have proposed a novel parametrization of a dark fluid, which may include both DM and DE. In the Sec. II, we have considered the barotropic equation of the state parameter $w(a)$ as a general polynomial function with

a scale factor as a variable. We have shown that the existence of a stationary point of $w(a)$ secures the lack of divergences of w in the far future. For a simple example of such a barotropic parameter with a stationary point, we have shown that it can describe the smooth transition between the initial zero barotropic parameter $w_i = 0$ and the negative DE equation of state parameter $w_{de} < -1/3$; therefore, it may be used to unify DM and DE in one dark fluid.

In the Sec. III, we have investigated the DF parametrization in two cases: for constant and dynamical energy density of the DE. We have included the constraints on the background evolution of the Universe using data from JLA supernovae, BAO, CMB, BBN, and Hubble expansion. We have implemented the MCMC statistical analysis for the two considered DE scenarios, and we compared the results with the ΛCDM model. We have proven that both DF parametrizations are well fitted to observations as equally as the concordance ΛCDM model. For all considered

models, we have also founded the redshift, for which the Universe starts to accelerate. The results vary from $z_{tr} = 0.9$ (for the case 1) to $z_{tr} = 0.66$ for the ΛCDM, all in good agreement with recent works [72–74,78].

In the Sec. IV, we have investigated the growth rate of matter perturbations in the context of unified DF cosmology. We have shown that in this model the DE component, like Λ sector in the standard ΛCDM model, can suppress the amplitude of matter perturbations at low redshift while its effects on the growth rate are negligible at high redshift epochs. We have also proven that both cases of DF parametrization are consistent with growth rate data in cluster scales as equally as the concordance ΛCDM model.

ACKNOWLEDGMENTS

[1] M. Persic, P. Salucci, and F. Stel, Mon. Not. R. Astron. Soc. **281,** 27 (1996).

[2] A. Borriello and P. Salucci, Mon. Not. R. Astron. Soc. **323,** 285 (2001).

[3] C. S. Frenk, A. E. Evrard, S. D. M. White, and F. J. Summers, Astrophys. J. **472,** 460 (1996).

[4] J. R. Primack, arXiv:astro-ph/9610078.

[5] P. A. R. Ade et al. (Planck), Astron. Astrophys. **594,** A13 (2016).

[6] A. G. Riess, A. V. Filippenko, P. Challis et al., Astron. J. **116,** 1009 (1998).

[7] S. Perlmutter, G. Aldering, G. Goldhaber et al., Astrophys. J. **517,** 565 (1999).

[8] M. Kowalski, D. Rubin, G. Aldering et al., Astrophys. J. **686,** 749 (2008).

[9] E. Komatsu, J. Dunkley, M. R. Nolta et al., Astrophys. J. Suppl. Ser. **180,** 330 (2009).

[10] E. Komatsu, K. M. Smith, J. Dunkley et al., Astrophys. J. Suppl. Ser. **192,** 18 (2011).

[11] N. Jarosik, C. L. Bennett, J. Dunkley, B. Gold, M. R. Greason, M. Halpern, R. S. Hill, G. Hinshaw, A. Kogut, E. Komatsu et al., Astrophys. J. Suppl. Ser. **192,** 14 (2011).

[12] M. Tegmark et al. (SDSS), Phys. Rev. D **69,** 103501 (2004).

[13] W. J. Percival, B. A. Reid, D. J. Eisenstein et al., Mon. Not. R. Astron. Soc. **401,** 2148 (2010).

[14] S. Cole et al. (2dFGRS Collaboration), Mon. Not. R. Astron. Soc. **362,** 505 (2005).

[15] D. J. Eisenstein et al. (SDSS Collaboration), Astrophys. J. **633,** 560 (2005).

[16] B. A. Reid, L. Samushia, M. White, W. J. Percival, M. Manera et al., Mon. Not. R. Astron. Soc. **426,** 2719 (2012).

[17] C. Blake, S. Brough, M. Colless, C. Contreras, W. Couch et al., Mon. Not. R. Astron. Soc. **415,** 2876 (2011).

[18] E. P. S. Shellard and R. A. Battye, Phys. Rep. **307,** 227 (1998).

[19] A. Falvard et al., Astropart. Phys. **20,** 467 (2004).

[20] A. Bottino, F. Donato, N. Fornengo, and P. Salati, Phys. Rev. D **72,** 083518 (2005).

[21] T. Appelquist, H.-C. Cheng, and B. A. Dobrescu, Phys. Rev. D **64,** 035002 (2001).

[22] L. Randall and R. Sundrum, Phys. Rev. Lett. **83,** 3370 (1999).

[23] S. Weinberg, Rev. Mod. Phys. **61,** 1 (1989).

[24] S. M. Carroll, Living Rev. Relativity **4,** 1 (2001).

[25] T. Padmanabhan, Phys. Rep. **380,** 235 (2003).

[26] E. J. Copeland, M. Sami, and S. Tsujikawa, Int. J. Mod. Phys. D **15,** 1753 (2006).

[27] R. R. Caldwell, R. Dave, and P. J. Steinhardt, Phys. Rev. Lett. **80,** 1582 (1998).

[28] E. Witten, arXiv:hep-ph/0002297.

[29] P. T. Silva and O. Bertolami, Astrophys. J. **599,** 829 (2003).

[30] V. Sahni, Pramana **55,** 43 (2000).

[31] A. Yu. Kamenshchik, U. Moschella, and V. Pasquier, Phys. Lett. B **511,** 265 (2001).

[32] M. C. Bento, O. Bertolami, and A. A. Sen, Phys. Rev. D **66,** 043507 (2002).

[33] I. Maor, R. Brustein, and P. J. Steinhardt, Phys. Rev. Lett. **86,** 6 (2001); **87,** 049901(E) (2001).

[34] A. G. Riess et al. (Supernova Search Team), Astrophys. J. **607,** 665 (2004).

[35] M. Chevallier and D. Polarski, Int. J. Mod. Phys. D **10,** 213 (2001).

[36] E. V. Linder, Phys. Rev. Lett. **90,** 091301 (2003).

[37] H. K. Jassal, J. S. Bagla, and T. Padmanabhan, Mon. Not. R. Astron. Soc. **356,** L11 (2005).

[38] E. M. Barboza, J. S. Alcaniz, Z. H. Zhu, and R. Silva, Phys. Rev. D **80,** 043521 (2009).

[39] G. Efstathiou, Mon. Not. R. Astron. Soc. **310,** 842 (1999).

[40] C. Wetterich, Phys. Lett. B **594,** 17 (2004).

[41] M. Artymowski, Z. Lalak, and M. Lewicki, J. Cosmol. Astropart. Phys. 01 (2017) 011.

[42] J. J. M. Carrasco, R. Kallosh, and A. Linde, Phys. Rev. D **92,** 063519 (2015).

[43] K. Dimopoulos and C. Owen, J. Cosmol. Astropart. Phys. 06 (2017) 027.

[44] L. H. Ford, Phys. Rev. D **35,** 2955 (1987).

[45] T. Kunimitsu and J. Yokoyama, Phys. Rev. D **86,** 083541 (2012).

[46] The case of the transition between $w = 1/3$ and $w = -1$ can be realized for the K-essence [79].

[47] G. Hinshaw et al. (WMAP), Astrophys. J. Suppl. Ser. **208,** 19 (2013).

[48] L. Amendola, Phys. Rev. D **62,** 043511 (2000).

[49] S. del Campo, R. Herrera, G. Olivares, and D. Pavon, Phys. Rev. D **74,** 023501 (2006).

[50] V. Poitras, Gen. Relativ. Gravit. **46,** 1732 (2014).

[51] H. Sandvik, M. Tegmark, M. Zaldarriaga, and I. Waga, Phys. Rev. D **69,** 123524 (2004).

[52] R. J. F. Marcondes, R. C. G. Landim, A. A. Costa, B. Wang, and E. Abdalla, J. Cosmol. Astropart. Phys. 12 (2016) 009.

[53] W. Yang, L. Xu, Y. Wang, and Y. Wu, Phys. Rev. D **89,** 043511 (2014).

[54] M. Betoule et al. (SDSS), Astron. Astrophys. **568,** A22 (2014).

[55] C. Escamilla-Rivera, L. Casarini, J. C. Fabris, and J. S. Alcaniz, J. Cosmol. Astropart. Phys. 11 (2016) 010.

[56] F. Beutler, C. Blake, M. Colless, D. H. Jones, L. Staveley-Smith, G. B. Poole, L. Campbell, Q. Parker, W. Saunders, and F. Watson, Mon. Not. R. Astron. Soc. **423,** 3430 (2012).

[57] X. Xu, A. J. Cuesta, N. Padmanabhan, D. J. Eisenstein, and C. K. McBride, Mon. Not. R. Astron. Soc. **431,** 2834 (2013).

[58] L. Anderson et al. (BOSS), Mon. Not. R. Astron. Soc. **441,** 24 (2014).

[59] D. L. Shafer and D. Huterer, Phys. Rev. D **89,** 063510 (2014).

[60] P. Serra, A. Cooray, D. E. Holz, A. Melchiorri, S. Pandolfi, and D. Sarkar, Phys. Rev. D **80,** 121302 (2009).

[61] M. Moresco et al., J. Cosmol. Astropart. Phys. 08 (2012) 006.

[62] E. Gaztanaga, A. Cabre, and L. Hui, Mon. Not. R. Astron. Soc. **399,** 1663 (2009).

[63] A. Mehrabi, S. Basilakos, and F. Pace, Mon. Not. R. Astron. Soc. **452,** 2930 (2015).

[64] S. Basilakos, M. Plionis, and J. Sola, Phys. Rev. D **80,** 083511 (2009).

[65] A. Mehrabi, S. Basilakos, M. Malekjani, and Z. Davari, Phys. Rev. D **92,** 123513 (2015).

[66] A. Mehrabi, F. Pace, M. Malekjani, and A. Del Popolo, Mon. Not. R. Astron. Soc. **465,** 2687 (2017).

[67] M. Malekjani, S. Basilakos, Z. Davari, A. Mehrabi, and M. Rezaei, Mon. Not. R. Astron. Soc. **464,** 1192 (2017).

[68] J. Sol, A. Gmez-Valent, and J. de Cruz Prez, Astrophys. J. **836,** 43 (2017).

[69] H. Akaike, IEEE Trans. Autom. Control **19,** 716 (1974).

[70] N. Sugiura, Commun. Stat., Theory Methods **7,** 13 (1978).

[71] G. Schwarz, Ann. Stat. **6,** 461 (1978).

[72] O. Farooq, F. R. Madiyar, S. Crandall, and B. Ratra, Astrophys. J. **835,** 26 (2017).

[73] S. Capozziello, O. Farooq, O. Luongo, and B. Ratra, Phys. Rev. D **90,** 044016 (2014).

[74] S. Capozziello, O. Luongo, and E. N. Saridakis, Phys. Rev. D **91,** 124037 (2015).

[75] M. C. Bento, O. Bertolami, and A. A. Sen, Phys. Rev. D **70,** 083519 (2004).

[76] D. Duniya, D. Bertacca, and R. Maartens, J. Cosmol. Astropart. Phys. 10 (2013) 015.

[77] S. Nesseris, G. Pantazis, and L. Perivolaropoulos, Phys. Rev. D **96,** 023542 (2017).

[78] M. Rezaei, M. Malekjani, S. Basilakos, A. Mehrabi, and D. F. Mota, Astrophys. J. **843,** 65 (2017).

[79] L. Garcia, J. Tejeiro, and L. Castaneda, arXiv:1210.5259.